Elucidation of the Complex Baylis-Hillman Reaction of 3-Methoxy-2-nitrobenzaldehyde with Methyl Vinyl Ketone

Kenudi C. Idahosa, Duduzile M. Molefe, Vusumzi E. Pakade, Michael E. Brown and Perry T. Kaye*

Department of Chemistry and Centre for Chemico- and Biomedicinal Research, Rhodes University, Grahamstown, 6140, South Africa.

ABSTRACT

DABCO-catalyzed reaction of 3-methoxy-2-nitrobenzaldehyde with methyl vinyl ketone (MVK) affords a mixture of products, comprising the 'normal' Baylis-Hillman adduct, the MVK dimer and a pair of diastereomeric bis-(MVK)Baylis-Hillman adducts. ^{1}H NMR spectroscopy-based kinetic studies have provided clear insights into the competing pathways and product distribution in this complex reaction.

KEYWORDS

Baylis-Hillman reaction, mechanism, kinetics, ^{1}H NMR spectroscopic analysis, bis-(MVK)Baylis-Hillman products.

1. Introduction

During recent years, interest in applications of Baylis-Hillman methodology in the construction of various molecular targets has grown enormously – as evidenced by comprehensive reviews by Basavaiah[1,2] and others.[3] Our own ongoing research has been concerned with both mechanistic[4] and synthetic aspects of this important reaction, with particular emphasis on its application in the preparation of heterocyclic systems.[5] We had found that reductive cyclization of 2-nitrobenzaldehyde-derived Baylis-Hillman adducts provided access to quinoline and quinolone derivatives,[6,7] but also observed various side reactions. These included formation of the diastereomeric bis-methyl vinyl ketone (MVK) adducts **5a**$_{syn}$ and **5b**$_{anti}$ as the major products (60 %), together with the normal Baylis-Hillman product **3a** (24 %) and the MVK dimer **4**, from reaction of 3-methoxy-2-nitrobenzaldehyde **1a** with MVK **2** (Scheme 1).[8]

While formation of the MVK dimer **4** is well known,[9] we had never previously encountered bis-MVK adducts, such as **5a**$_{syn}$ and **5b**$_{anti}$, in our use of the Baylis-Hillman reaction although evidence of conjugate addition of methyl acrylate to Baylis-Hillman-derived coumarins and chromenes was observed in an earlier study.[10] A search of the literature, however, revealed that Shi *et al.*[9,11,12] had, in fact, reported the formation of a series of such adducts, together with the corresponding 'normal' Baylis-Hillman products, when certain arylaldehydes – *but not* 2-nitrobenzaldehyde **1b** – were reacted with MVK **2** and 1,4-diazabicyclo[2.2.2]octane (DABCO) in CH$_2$Cl$_2$, DMF or DMSO. Shi *et al.*[11] considered two possible mechanistic pathways (corresponding to Paths **I** and **II** in Scheme 2) for the formation of the bis-MVK adducts, but favoured Path **I** because 2-nitrobenzaldehyde failed to react with the MVK dimer **2** in the presence of DABCO. Whether the failure of this latter reaction provides sufficient reason to exclude Path **II** or why bis-MVK adducts, such as **5a**$_{syn}$ and **5b**$_{anti}$, are formed from 3-methoxy-2-nitrobenzaldehyde **1a** but not from 2-nitrobenzaldehyde **1b** are clearly questions that need to be addressed. Kinetic-mechanistic and theoretical studies of the DABCO-catalyzed reactions of 3-methoxy-2-nitrobenzaldehyde **1a** with

MVK **4** were consequently initiated and, in this paper, we report the results of the former study.[13]

2. Results and Discussion

Flash chromatography of the crude material obtained from reacting 3-methoxy-2-nitrobenzaldehyde **1a**, MVK **2** and DABCO for 24 hours yielded the normal Baylis-Hillman product **3a** and a mixture of the *syn*-and *anti*-diastereomers **5a**$_{syn}$ and **5a**$_{anti}$, which were separated, in turn, by semi-preparative HPLC. The *syn* and *anti* configurational assignments by Shi *et al.*[11] were based on the relative magnitudes of the vicinal coupling constants (^3J_H) between the 3- and 4-protons (Fig. 1). In the present study, vicinal coupling (^3J_H), NOE and modelling data were all explored in order to confirm the stereochemical assignments. In the event, the ^3J_H values for the diastereomeric bis-MVK adducts proved to be comparable (4.56 and 5.46 Hz), while their NOESY spectra failed to reveal any structurally significant correlations. Consequently, the three staggered conformations of each diastereomer were geometry-optimized at the B3LYP/6-31G+(d) level using Gaussian03.[14] Examination of the relative energies of these rotamers indicated a clear preference for the staggered conformation **I** for **5a**$_{syn}$ and **II** for **5a**$_{anti}$, both of which appear to be stabilized by intramolecular hydrogen-bonding, as illustrated in Fig. 1. The similarity of the dihedral angles ($\Phi_{3H,4H}$: 60.4° for **I** and 65.6° for **II**) are consistent with the small, comparable ^3J_H values observed for each product. The relative energies of the staggered rotamers of the *anti*-adduct are, in fact, consistently lower than energies of the corresponding rotamers for the *syn*-adduct, permitting identification of the more stable product as the **5a**$_{anti}$ adduct. Moreover, the calculated difference ($\Delta G°$ *ca.* 1.0 kJ mol^{-1}) between the energies of the most stable rotamers of the **5a**$_{syn}$ and **5a**$_{anti}$ adducts corresponds to an equilibrium constant, K = *ca.* 1.5 at 298 K – a value consistent with the experimental concentrations (0.31:0.24 = 1.3 at 298 K) after *ca.* 50 000 s.

It was hoped that the vinylic methylene proton signals for each species (**1a**, **2**, **3a**, **5a**$_{syn}$ and **5a**$_{anti}$) could be used to monitor the progress of the reaction, but signal overlap in the vinylic region made this impracticable – even with the application of a

* To whom correspondence should be addressed. E-mail: p.kaye@ru.ac.za

Scheme 1
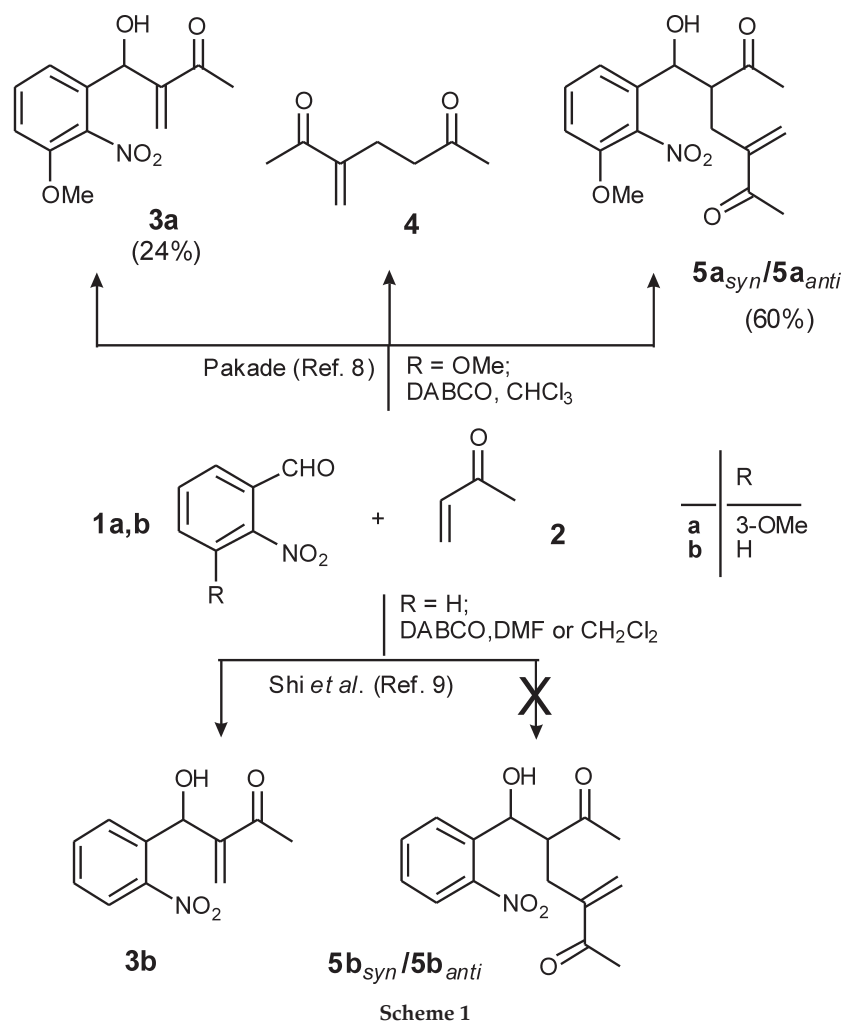
deconvolution method[15] to enhance peak resolution. The use of ^{13}C NMR spectroscopy was explored, but it became apparent that, even after a 50 s delay (corresponding to T_1 = 72.2 s), the vinylic methylene carbon signals had not relaxed completely, and the need for multiple acquisitions effectively precluded use of ^{13}C NMR spectroscopy. Finally, various ^{1}H NMR signals were identified which correspond uniquely to the reactants (**1a** and **2**) and products (**3a**, **4**, **5a**$_{syn}$ and **5a**$_{anti}$) and the kinetic studies were successfully conducted on an NMR-tube scale, using 1,3,5-trimethoxybenzene as an internal standard.

Possible routes (following Shi *et al.*[11]) to the products isolated in our study are outlined in Scheme 2, and analysis of the kinetic data was simplified by using the diagrams in Fig. 2. The initial concentrations of the reactants were known, and the spectroscopic integral data could be used to calculate reactant and product concentrations at regular intervals. However, by the time the first NMR spectrum was recorded, the concentration of aldehyde **1a** had decreased significantly from the initial 0.7305 mol L^{-1} and it was necessary to introduce a time correction This was determined by extrapolation of the approximately linear (r^2 = 0.974) first-order plot of – ln[**1a**] *vs.* time (Fig. 3) and use of Equation 1, where k_I and k_{II} are the rate constants for the putative reactions involving **1a** in path **I** and path **II**, respectively. Substitution of the rate constant for the disappearance of **1a** [$k_a = (k_I + k_{II}) = 4.74 \times 10^{-4}$ s^{-1}] and the intercept (0.5129 mol L^{-1}) from Fig. 3 into Equation 1 afforded Equation 2 and, thence, the time correction (t_{corr} = –420 s).

$$-\ln [\mathbf{1a}] = (k_I + k_{II})t - \ln[\mathbf{1a}]_0 \qquad (1)$$

$$-\ln [\mathbf{1a}] = 4.74 \times 10^{-4}\, t + 0.5129 \qquad (2)$$

Since $\quad -\ln [\mathbf{1a}] = -\ln [0.7305] = 0.3140$

and $\quad 0.3140 = 4.74 \times 10^{-4}\, t_{corr} + 0.5129$

$$t_{corr} = -(0.5129 - 0.3140)/4.74 \times 10^{-4} = -420 \text{ s}$$

The time-corrected plot of the changes in concentration of reactants and products, illustrated in Fig. 4, reflects the consumption of the substrate, 3-methoxy-2-nitrobenzaldehyde **1a** and the formation of four products **3a**, **4**, **5a**$_{syn}$ and **5a**$_{anti}$. After *ca.* 10 000 s, the substrate **1a** is completely consumed, while the normal Baylis-Hillman product **3a** and the *syn*-adduct **5a**$_{syn}$ reach maximum concentrations of 0.24 and 0.26 mol L^{-1}, respectively. Thereafter, the normal product **3a** undergoes gradual, apparent zero-order decay, the linear decrease in the experimental data coinciding with the straight line constructed using Equation 3 (Fig. 5).

$$[\mathbf{3a}] = [\mathbf{3a}]_{10000s}\ k_{3a}t \qquad (3)$$

where k_{3a} = –2.66 × 10^{-6} mol L^{-1} s^{-1} and [**3a**]$_{10000\ s}$ = 0.24 mol L^{-1}.

The concentration of the MVK dimer **4** also increases steadily with time. The activated alkene, MVK **2**, is consumed rapidly at the beginning of the reaction, but its rate of consumption gradually decreases as the reaction proceeds. The rapid, initial consumption of the MVK **2** can be attributed to its simultaneous involvement in the formation of four products (**3a**, **5a**$_{syn}$, **5a**$_{anti}$ and **4**) but, after *ca.* 10000 s and the complete consumption of the aldehyde **1a**, MVK **2** is only required for the continued formation of the MVK dimer **4** and, possibly, for the conversion of the

Scheme 2
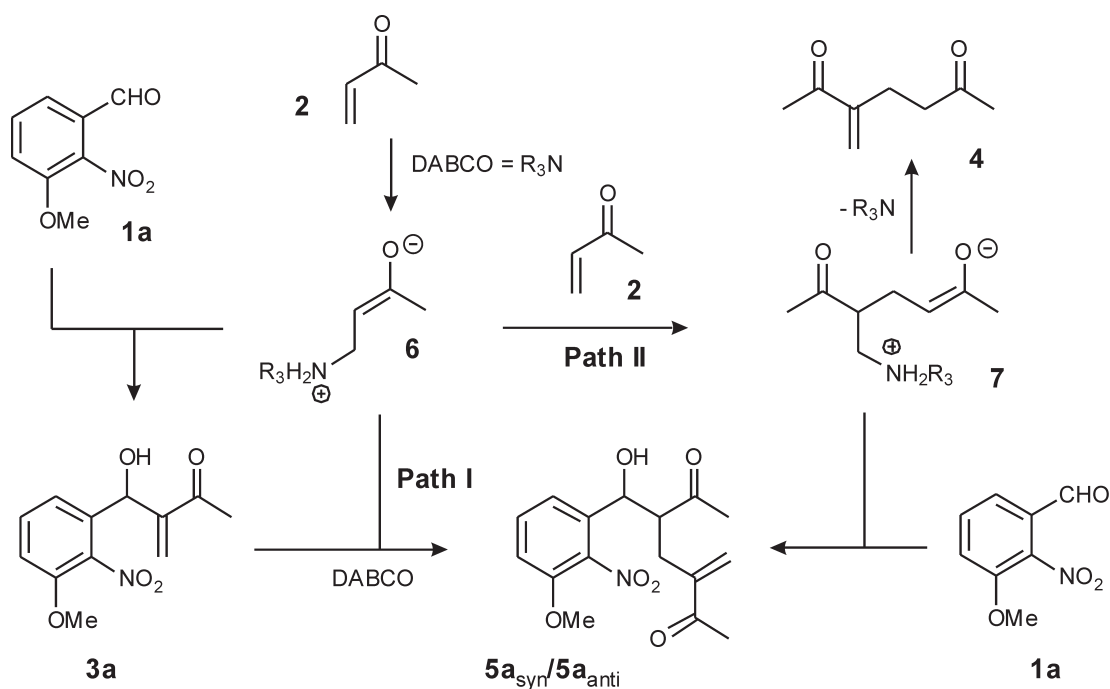
Competing pathways for the formation of the 'normal' Baylis-Hillman adduct **3a** and the diastereomeric bis-MVK Baylis-Hillman adducts **5a**$_{syn}$ and **5a**$_{anti}$.

normal Baylis-Hillman product **3a** to the bis-MVK adducts **5a**$_{syn}$ and **5a**$_{anti}$ *via* Path **I**. The formation of the MVK dimer **4** is expected to follow third-order kinetics, i.e. Rate = k_4[**2**]^2[DABCO] but, since the catalyst concentration [DABCO] is constant, it should exhibit pseudo second-order kinetics – an expectation confirmed by analysis of the experimental data (after *ca.* 10 000 s), which affords a pseudo-second-order rate constant of 3.97×10^{-6} L mol^{-1} s^{-1} ($r^2 = 0.975$). The *total* concentration (*ca.* 0.695 ± 0.035 mol L^{-1}) of the substrate **1a** and the substrate-derived products **3a**, **5a**$_{syn}$ and **5a**$_{anti}$ remains relatively constant for the duration of the reaction and corresponds to the *initial* concentration of the aldehyde **1a** (0.7305 mol L^{-1}) implying the absence of any significant competing reactions.

It might be presumed *a priori* that the diastereomeric bis-MVK adducts **5a**$_{syn}$ and **5a**$_{anti}$ could be formed, at least initially,

via both routes, *viz.* Path **I**, in which 3-methoxy-2-nitro-benzaldehyde **1a** is converted to the adducts *via* the normal Baylis-Hillman product **3a**, and Path **II**, in which they are formed directly by reaction between the aldehyde **1a** and the bis-MVK zwitterion **7**. It might also be presumed that, after *ca.* 10 000 s (by which time the substrate **1a** has been consumed), the only viable pathway would be Path **I**, which makes use of the available Baylis-Hillman product **3a**. However, for the following reasons, we have been led to somewhat different conclusions.

i) If Path **I** alone is followed, the rate of formation of the bis-MVK adducts should be greatest when the concentration of the normal Baylis-Hillman adduct **3a** is highest, i.e. at *ca.* 10 000 s, but the opposite is observed; the rate of formation of the bis-MVK adducts (**5a**$_{total}$ = **5a**$_{syn}$ + **5a**$_{anti}$) actually *decreases* significantly after this time. In fact, the rate of forma-
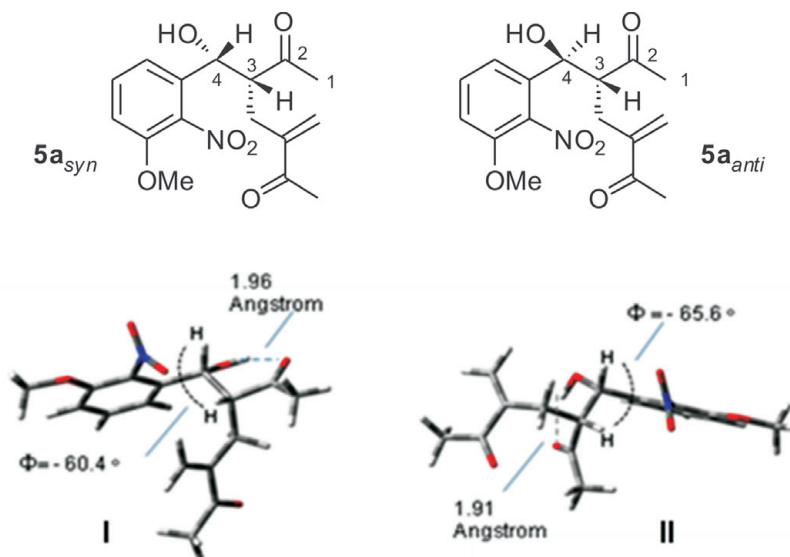

Figure 1 Line drawings and computer-modelled structures of the lowest energy staggered rotamers of the diastereomeric bis-MVK adducts **5a**$_{syn}$ and **5a**$_{anti}$.
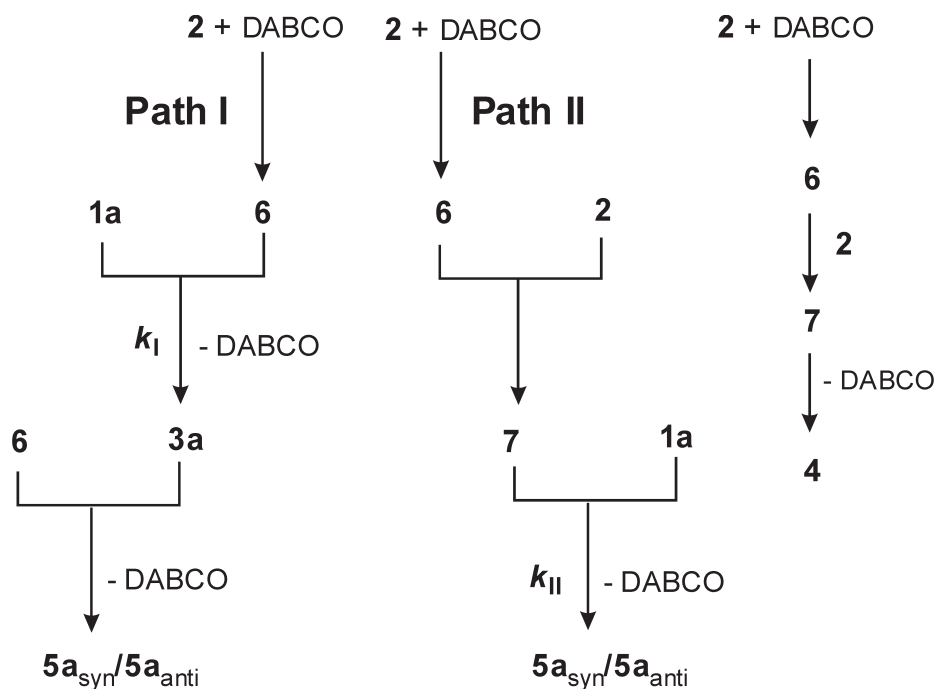
Figure 2 Simplified schematic diagram illustrating possible reaction pathways (*cf.* Scheme 2).

tion of the more stable bis-MVK adduct $5a_{anti}$ decreases long before [$3a$] reaches its maximum, suggesting that reaction *via* Path **I**, if occurring at all, is significantly slower than Path **II**.

ii) Path **II** depends directly on the availability of the substrate **1a**, the concentration of which is greatest in the initial phase of the reaction (<10 000 s) – the phase in which the rate of formation of the bis-MVK adducts ($5a_{total} = 5a_{syn} + 5a_{anti}$) is also greatest!

The failure of 2-nitrobenzaldehyde **1b** to react with the MVK dimer **4** in the presence of DABCO understandably prompted Shi *et al.*[11] to preclude Path **II** from consideration. Our attempt to react 3-methoxy-2-nitrobenzaldehyde **1a** under similar conditions also proved unsuccessful (Scheme 3). However, Path **II** requires the zwitterionic enolate **7** (Scheme 2) whereas, once formed, the MVK dimer **4** would be expected to react with DABCO to form the zwitterion **8** not the isomeric

system **7** (Scheme **4**). The former, α,α-disubstituted enolate species **8** cannot undergo a Baylis-Hillman type reaction and, consequently, unless the isomerization **8 → 7** occurs readily, the MVK dimer **4** cannot participate *per se* in the formation of the bis-MVK adducts $5a_{syn}$ and $5a_{anti}$. On the other hand, the DABCO-catalyzed reaction of the Baylis-Hillman adduct **3a** with MVK **4** was found to proceed, but *very slowly* (Scheme 3). Thus, while reaction *via* Path **I** may contribute, we conclude that Path **II** represents the dominant reaction pathway for the formation of the bis-MVK adducts $5a_{syn}$ and $5a_{anti}$ during the initial phase of the reaction (<10 000 s).

In the initial stage of the reaction the product distribution is essentially kinetically-controlled and at *ca.* 10 000 s, [$5a_{syn}$]> [$3a$]>[$5a_{anti}$]; after this time, however, the substrate concentration [$1a$] = 0 and [$5a_{syn}$] and [$3a$] both decrease while [$5a_{anti}$] increases. The final product distribution is thus thermodynamically-
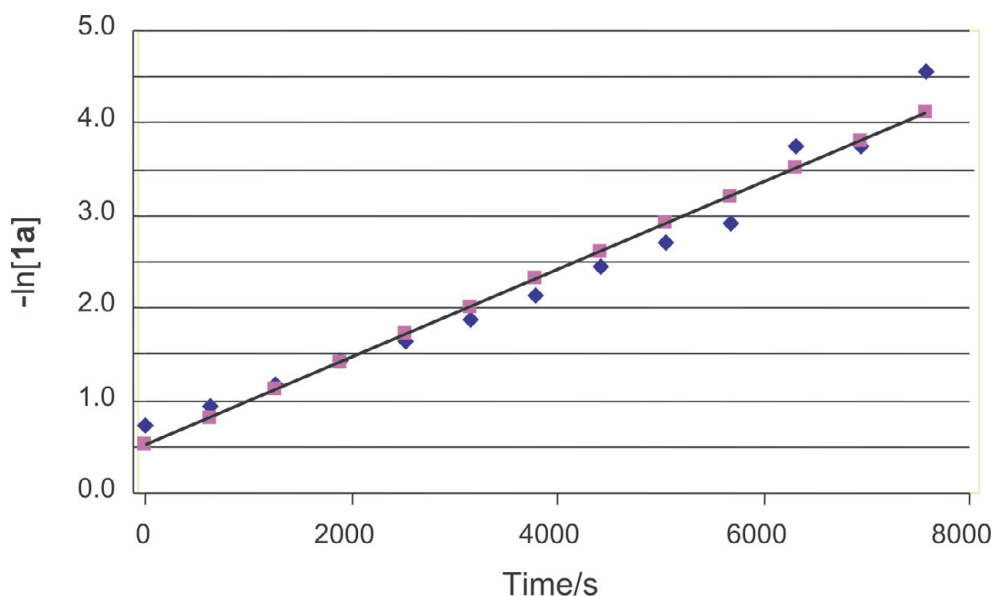

Figure 3 Time-corrected experimental (■) and calculated (◆) first-order plots of –ln[**1a**] against time for the consumption of 3-methoxy-2-nitrobenzaldehyde **1a**.
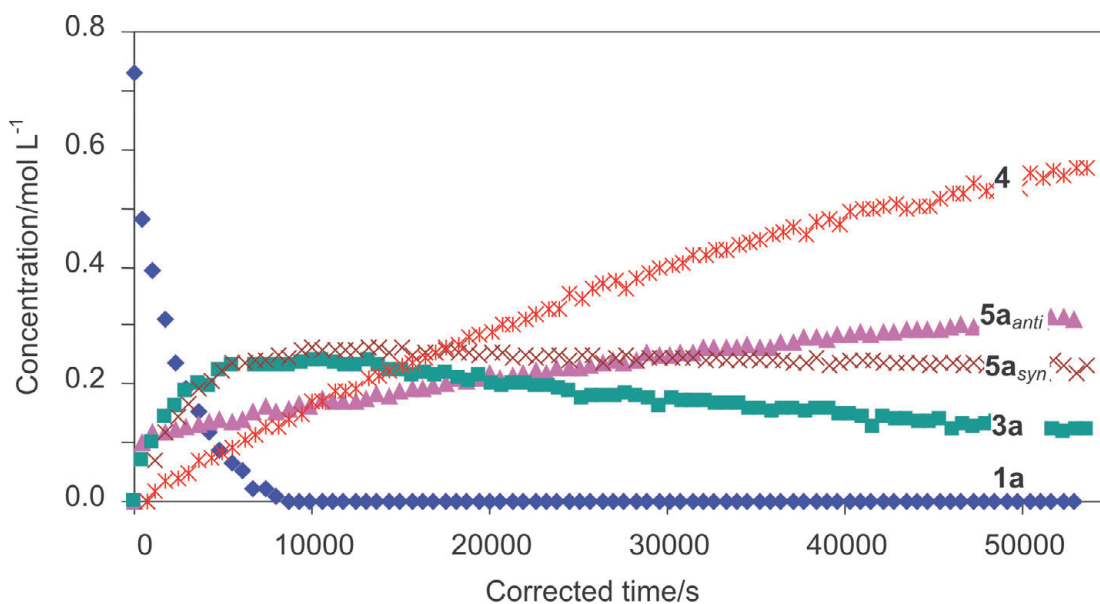
Figure 4 Time-corrected plots of the changes in concentrations of 3-methoxy-2-nitrobenzaldehyde **1a**, the Baylis-Hillman product **3a**, the bis-MVK adducts **5a**$_{syn}$ and **5a**$_{anti}$ and the MVK dimer **4** during the reaction.

controlled, with the more stable adduct **5a**$_{anti}$ being produced at the expense of both the normal Baylis-Hillman product **3a** and the bis-MVK adduct **5a**$_{syn}$. At *ca.* 50 000 s, the system appears to approach equilibrium, and a lower limit may be calculated for the equilibrium constant, i.e. $K = [5a_{anti}]/[5a_{syn}] = 0.31/0.24 = 1.3$ at 298 K. The continued formation of **5a**$_{anti}$ after *ca.* 10 000 s can be attributed to a combination of slow consumption of the normal Baylis-Hillman product **3a** *via* Path **I** and isomerization of **5a**$_{syn}$ to **5a**$_{anti}$. It is noteworthy that the slow consumption of the normal adduct **3a** after *ca.* 10 000 s is comparable to the rate of formation of **5a**$_{total}$ and consistent with a slow Path **I** process. A putative DABCO-catalyzed pathway for the isomerization process (**5a**$_{syn}$ → **5a**$_{anti}$) is outlined in Scheme 5.

Plots of data in the approximately linear region (>10 000 s; Fig. 4) afford slopes and intercepts and, hence, rate constants for the formation of **5a**$_{anti}$ and the consumption of **5a**$_{syn}$ and **3a** (Table 1). The reaction using the aldehyde **1a** was repeated at various temperatures (295–315 K) with the intention of accessing activation energy data. However, no consistent trends were observed. This is, perhaps, not surprising given the complexity of the transformation and the reversibility of the various steps.

The electrophilicity of the aldehydic carbon in 2-nitro-benzaldehyde **1b** should be *enhanced* by the electron-with-

drawing effect of the *ortho*-nitro group (Fig. 6a), and rapid attack by the MVK zwitterion **6** (in preference to the sterically hindered and, hence, less nucleophilic bis-MVK zwitterion **7**), would explain formation of the 'normal' Baylis-Hillman adduct **3b** as a *kinetically-controlled* product. In the case of 3-methoxy-2-nitrobenzaldehyde **1a**, however, the electron-withdrawing effect of the 2-nitro group is expected to be diminished by: i) 'cross-conjugation' involving delocalization the 3-methoxy group lone-pair electrons (Fig. 6b); and ii) sterically induced rotation of the 2-nitro group (evident in Fig. 1). The *decrease* in the electrophilicity of the aldehydic carbon in 3-methoxy-2-nitrobenzaldehyde **1a** (and, consequently, the reaction rate), coupled with the reversibility of the reactions, would account for the competitive formation of the *thermodynamically-favoured* bis-MVK adducts **5a**$_{syn}$ and **5a**$_{anti}$, particularly in the presence of excess MVK.

2. Experimental

2.1. Kinetic Studies

^{1}H-NMR spectroscopic data were obtained on a Bruker Avance 400 MHz spectrometer at 298 K. The substrate, 3-methoxy-2-nitrobenzaldehyde **1a**, was placed, together with trimethoxy-
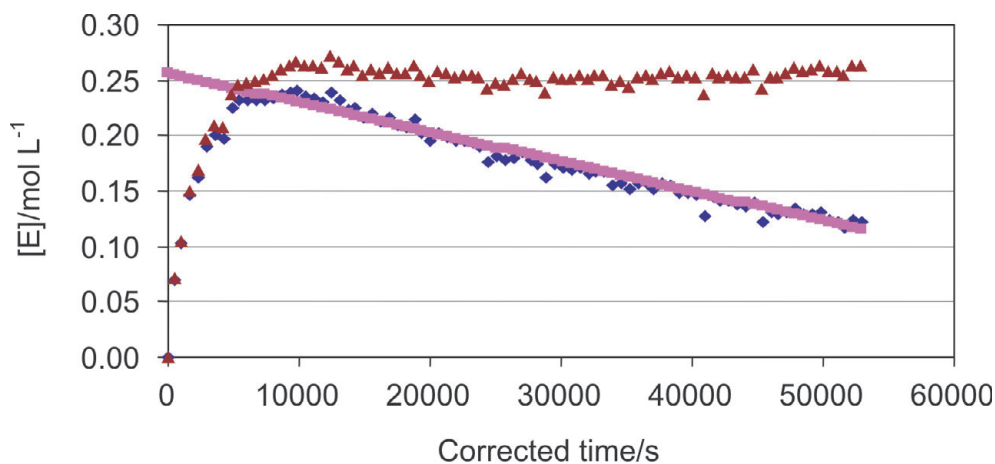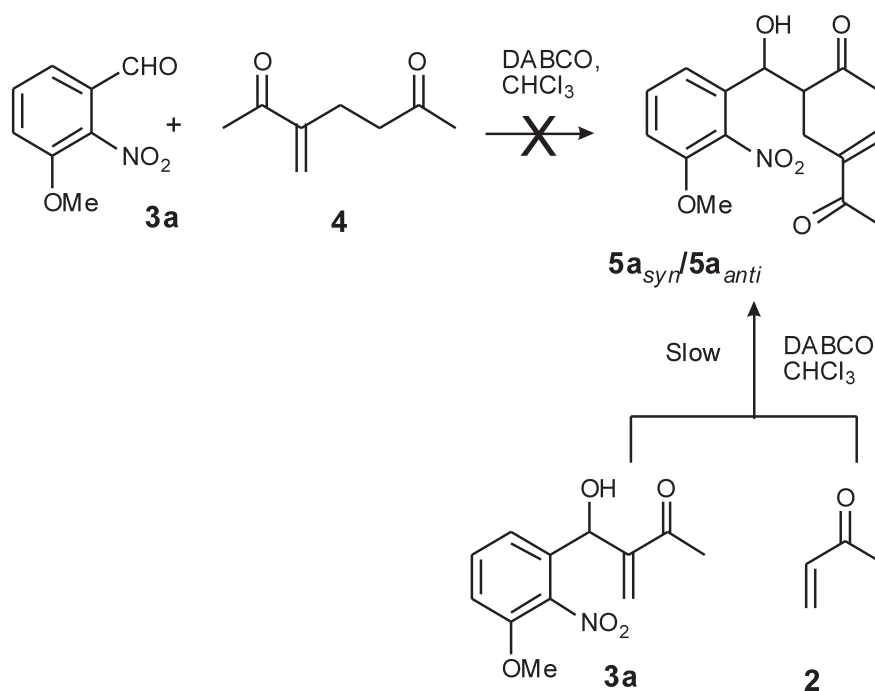

Figure 5 Plot showing the formation and disappearance of product **3a** with time. [(♦) indicates the experimental [**3a**], (■) the zero-order plot for the consumption of **3a** and (▲) the expected concentration [**3a**] in the absence of the zero-order reaction.

Scheme 3

Table 1 Kinetic data for the approximately linear region (Figure 4) after *ca.* 10 000 s at 298 K.

Component	Rate constant/L mol^{-1}s^{-1}	Concentration at t = 10 000 s /mol L^{-1}
5a$_{total}$	2.8×10^{-6}	0.42
5a$_{anti}$	3.5×10^{-6}	0.16
5a$_{syn}$	-2.1×10^{-6}	0.26
3a	-2.7×10^{-6}	0.24

benzene and 1,4-diazabicyclo[2.2.2]octane (DABCO), in a 1 mL graduated NMR tube, and CDCl$_3$ was then added. After complete dissolution (*ca.* 5 min), methyl vinyl ketone (MVK) was added to bring the total volume of the solution to 1.0 mL. The initial spectrum was run as soon as possible and subsequent spectra were run at 10 min intervals for a period of 14 h. The data obtained were converted into concentrations by using trimethoxybenzene as an internal standard.

In a typical experiment, MVK (0.370 mL, 4.44 mmol) was added to a solution of 3-methoxy-2-nitrobenzaldehyde **1a** (0.119 g,

Scheme 4

0.657 mmol), trimethoxybenzene (0.0172 g, 0.105 mmol), DABCO (0.0353 g, 0.315 mmol) and CDCl$_3$ (0.53 mL). The experiment was conducted three times, affording comparable results.

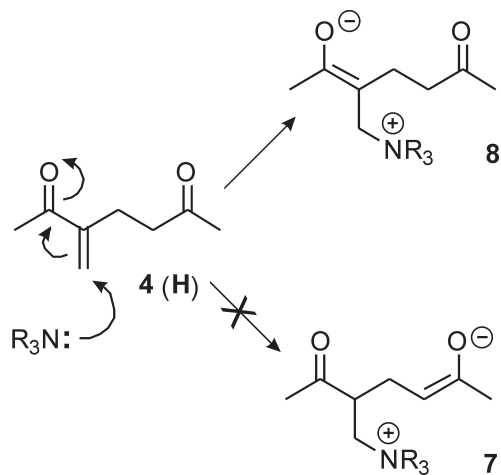## 2.2. Reaction of 3-methoxy-2-nitrobenzaldehyde with MVK and DABCO

A solution of 3-methoxy-2-nitrobenzaldehyde **1a** (2.35 g, 13.0 mmol), MVK (1.90 mL, 22.8 mmol), DABCO (0.70 g, 0.65 mmol) in CHCl$_3$ (3 mL) was stirred at r.t. in a stoppered flask for *ca.* 48 h, and the progress of reaction was monitored by TLC. Excess solvent and unreacted MVK were evaporated from the crude mixture *in vacuo,* and the residue was purified by flash chromatography on silica gel [elution with EtOAc-hexane (1:3)] to afford two fractions.

Fraction 1. 4-Hydroxy-4-(3-methoxy-2-nitrophenyl)-3-methylenebutan-2-one **3a**, as a viscous, light-brown transparent oil (1.30 g; 40 %), (lit.[16] cited as oil).

Fraction 2. A dark brown oil (*ca.* 20 %) comprising a mixture of the *syn* and *anti* diastereomers, HPLC of which [using a Whatman Partisil 10 column and eluting with EtOAc-hexane (1:1)] gave:

i) the *syn*-diastereomer, *5-acetyl-6-hydroxy-6-(3-methoxy-2-nitrophenyl)-3-methylene-2-hexanone* **5a**$_{syn}$ [(Found M+23: 344.1099. Calc. for C$_{16}$H$_{19}$NO$_6$Na: 344.1110); ν_{max} (ATR)/cm^{-1} 3412 (OH), 1706 and 1671 (2 × C=O); δ_H (400 MHz; CDCl$_3$) 2.07 and 2.24 (6H, 2 × s, 2 × CH$_3$CO), 2.61 (2H, m, CH$_2$), 3.21 (1H, m, C*H*CH$_2$), 3.38 (1H, br s, OH), 3.87 (3H, s, OCH$_3$), 5.00 (1H, d, *J* = 4.56 Hz,[†] C*H*OH), 5.68 and 5.94 (2H, 2 × s, C=CH$_2$), 6.97 (1H, d, *J* = 8.0 Hz, Ar-H), 7.17 (1H, d, *J* = 8.0 Hz, Ar-H) and 7.40 (1H, t, *J* = 8.2 Hz, Ar-H); δ_C (100 MHz; CDCl$_3$) 25.7 (CH$_3$CO), 27.5 (CH$_2$), 31.1 (CH$_3$CO), 55.6 (CHCH$_2$), 56.5 (OCH$_3$), 68.8 (CHOH), 112.0 and 119.9 (Ar-C), 127.6 (C=CH$_2$), 130.9 (*C*=CH$_2$), 134.2, 139.9, 146.0 and 150.9 (*C*=CH$_2$ and Ar-C) , 199.5 and 211.6 (2 × C=O)]; and

ii) the *anti*-diastereomer, *5-acetyl-6-hydroxy-6-(3-methoxy-2-nitrophenyl)-3-methylene-2-hexan-one* **5a**$_{anti}$ [(Found M+23: 344.1111. Calc. for C$_{16}$H$_{19}$NO$_6$Na: 344.1110.); ν_{max} (ATR)/cm^{-1} 3427 (OH), 1709 and 1671 (2 × C=O); δ_H (600 MHz; CDCl$_3$) 2.07 and
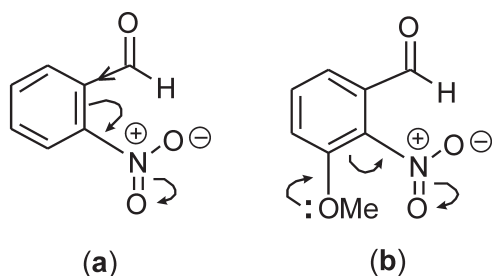

[†]From 600 MHz spectrum.
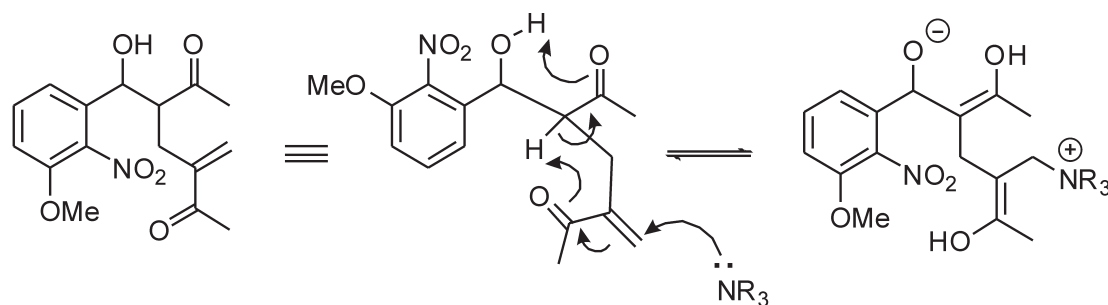
Scheme 5

Putative DABCO-catalyzed reaction permitting equilibration of the bis-MVK products $5a_{syn}$ and $5a_{anti}$.

Figure 6 Electron delocalization effects in (**a**) 2-nitrobenzaldehyde **1b**; and (**b**) 3-methoxy-2-nitrobenzaldehyde **1a**.

2.31 (6H, 2 × s, 2 × CH_3CO), 2.33 (1H, m, CHCH$_2$), 2.53 (1H, dd, J = 13.3 and 6.5 Hz, CHCH_A), 3.10 (1H, dd, J = 13.3 and 6.4 Hz, CHCH_B), 3.84 (3H, s, OCH_3), 3.86 (1H, d, J = 4.6 Hz, OH), 4.67 (1H, d, J = 5.46 Hz, CHOH), 5.84 and 6.05 (2H, 2 × s, C=CH$_2$), 6.94 (1H, d, J = 8.2 Hz, Ar-H), 7.08 (1H, d, J = 7.9 Hz, Ar-H) and 7.40 (1H, t, J = 8.1 Hz, Ar-H); δ_C (150 MHz; CDCl$_3$) 25.7 (CH$_3$CO), 30.8 (CH$_2$), 31.9 (CH$_3$CO), 54.9 (CHCH$_2$), 56.4 (OCH$_3$), 69.5 (CHOH), 111.8 and 118.8 (Ar-C), 128.7 (C=CH$_2$), 131.2 (Ar-C), 135.4 (*C*=CH$_2$), 140.0, 144.9 and 150.6 (Ar-C) , 199.3 and 213.2 (2 × C=O)].

Acknowledgements

References and Notes

1 D. Basavaiah, P.D. Rao and R.S. Hyma, *Tetrahedron,* 1996, **52**(24), 8001–8062.

2 D. Basavaiah, A.J. Rao and T. Satyanarayana, *Chem. Rev.,* 2003, **103**, 811–892.

3 (a) E. Ciganek, *Organic Reactions,* 1997, **51**, 203–350. (b) S.E. Drewes and G.H.P. Roos, *Tetrahedron,* 1988, **44**(15), 46563–4670.

4 (a) M.L. Bode and P.T. Kaye, *Tetrahedron Lett.,* 1991, **32,** 5611–5614. (b) P.T. Kaye, M.A. Musa, X.N. Nocanda and S. Robinson, *Org. Biomol. Chem.,* 2003, **1,** 1133–1138.

5 P.T. Kaye and X.W. Nocanda, *J. Chem. Soc., Perkin Trans. 1,* 2002, 1318–1323. P.T. Kaye, M.A. Musa and X.W. Nocanda, *Synthesis,* 2003, (4), 531–534.

6 O.B. Familoni, P.J. Klaas, K.A. Lobb, V.E. Pakade and P.T. Kaye, *Org. Biomol. Chem.,* 2006, **4**, 3960–3965.

7 O.B. Familoni, P.T. Kaye and P.J. Klaas, *J. Chem. Soc., Chem. Commun.,* 1998, 2563–2564.

8 V.E. Pakade, *Application of the Bayliss-Hillman Reaction in the Preparation of Quinoline Derivatives,* MSc thesis, Rhodes University, 2005.

9 M. Shi, C-Q. Li and J-K. Jiang, *Tetrahedron,* 2003, **59**, 1181–1185.

10 J. Bacsa, P.T. Kaye and R.S. Robinson, *S. Afr. J. Chem.,* 1998, **51**, 47–54.

11 M. Shi, C-Q. Li and J-K. Jiang, *Chem. Commun.,* 2001, 833–834.

12 M. Shi, C-Q. Li and J-K. Jiang, *Molecules,* 2002, **7**, 721–726.

13 The results of an ongoing theoretical study will be published in due course.

14 Gaussian 03, Revision E.01, M.J. Frisch, G.W. Trucks, H.B. Schlegel, G.E. Scuseria, M.A. Robb, J.R. Cheeseman, J.A. Montgomery, Jr., T. Vreven, K.N. Kudin, J.C. Burant, J.M. Millam, S.S. Iyengar, J. Tomasi, V. Barone, B. Mennucci, M. Cossi, G. Scalmani, N. Rega, G.A. Petersson, H. Nakatsuji, M. Hada, M. Ehara, K. Toyota, R. Fukuda, J. Hasegawa, M. Ishida, T. Nakajima, Y. Honda, O. Kitao, H. Nakai, M. Klene, X. Li, J.E. Knox, H.P. Hratchian, J.B. Cross, V. Bakken, C. Adamo, J. Jaramillo, R. Gomperts, R.E. Stratmann, O. Yazyev, A.J. Austin, R. Cammi, C. Pomelli, J.W. Ochterski, P.Y. Ayala, K. Morokuma, G.A. Voth, P. Salvador, J.J. Dannenberg, V.G. Zakrzewski, S. Dapprich, A.D. Daniels, M.C. Strain, O. Farkas, D.K. Malick, A.D. Rabuck, K. Raghavachari, J.B. Foresman, J.V. Ortiz, Q. Cui, A.G. Baboul, S. Clifford, J. Cioslowski, B.B. Stefanov, G. Liu, A. Liashenko, P. Piskorz, I. Komaromi, R.L. Martin, D.J. Fox, T. Keith, M. A. Al-Laham, C.Y. Peng, A. Nanayakkara, M. Challacombe, P.M.W. Gill, B. Johnson, W. Chen, M.W. Wong, C. Gonzalez and J.A. Pople, Gaussian, Inc., Wallingford CT, **2004**.

15 H. Hu, Q.N. Van, V.A. Mandelshtam and A.J. Shaka, *J. Magn. Reson.,* 1998, **134**, 76–87.

16 Y. Peng, Q. Ding, Z. Li, G. Wang and J. Cheng, *Tetrahedron Lett.*, 2003, **44**, 3871–3875.